

MODELING AND ASSESSMENT OF EBR-II FUEL WITH THE US NRC's FAST FUEL PERFORMANCE CODE

K.J. GEELHOOD

*Pacific Northwest National Laboratory
902 Battelle Blvd. PO Box 999, Richland, WA 99352 USA*

I.E. PORTER

*United States Nuclear Regulatory Commission
11545 Rockville Pike, Rockville, Maryland 20852 USA*

ABSTRACT

FAST is the current NRC thermal-mechanical fuel performance code that is the next evolution of FRAPCON, containing transient capabilities from FRAPTRAN, with a modern code architecture. Also included in FAST is a flexible material properties library, where new material properties can be easily added, making it possible to model fuel that is different from the traditional UO₂ fuel/Zr-alloy cladding that its predecessor codes had typically been applied to. A study was performed to exercise this modularity to model EBR-II fuel performance. To accomplish this modeling, the sodium coolant option already in FAST was used and material properties and models for U-Pu-Zr fuel and HT9 cladding were added to FAST. A number EBR-II rods were selected and the results from FAST were compared to the data.

This paper will discuss the modeling that was performed including any assumptions that were made and areas of large uncertainty. The results are compared to relevant data and assessment is made of the overall uncertainty in the modeling of EBR-II fuel by FAST.

1. Introduction

The FRAPCON fuel performance code [1] has been used by the United States Nuclear Regulatory Commission (US NRC) for more than 20 years to perform independent analyses of vendor fuel codes and methods that are used to evaluate the performance of light water reactor (LWR) fuel relative to various safety analysis design limits. FAST (Fuel Analysis under Steady-State & Transient) [3] is the next evolution of FRAPCON, which was used for steady-state analyses, combined with the transient functionalities from FRAPTRAN [2].

Recent interest in new fuel types and in new reactor designs has prompted the US NRC to evaluate their independent analysis codes to determine if they could be applied to new fuel types and/or new reactor designs. In the case of fuel performance codes, FRAPCON, had been specifically written to evaluate UO₂ and MOX in zirconium based cladding in light and heavy water reactor conditions. However, FAST has been written with a much larger degree of flexibility and material properties and fuel performance models are contained in separate libraries which are designed to be swapped out for other material properties or models. As such, FAST provides a flexible platform for modeling new fuel in water reactors or new fuel in other reactor systems.

The goal of this effort is to demonstrate that various fuel rods that were irradiated in EBR-II can be modeled in FAST by adding the appropriate material properties and fuel performance models. EBR-II was a fast reactor with liquid sodium coolant. The fuel under consideration is metal (U-Zr and U-Pu-Zr) fuel with a liquid sodium gap and HT9 cladding. This paper will describe the properties and models that have been added to FAST and an assessment of the code predictions against the limited data available for these rods (fission gas release, cladding strain, and sodium heatup).

It is noted that the main body of the assessment of FAST is against light water reactor UO₂/Zr-alloy clad fuel, and the predictions of a new fuel type in a new reactor type will be subject to greater levels of uncertainty due to the relatively small database to assess the predictions against. Despite this greater uncertainty, FAST was used to perform a sample safety analysis using current US NRC best understanding of metal fuel performance to demonstrate initial capabilities that have been developed.

2. Metal Fuel Fast Reactor Irradiation and Modeling

A significant number of irradiations of metal fuel under fast reactor conditions has been performed in both the Experimental Breeder Reactor Number Two (EBR-II) and in the Fast Flux Test Facility (FFTF) in the 1980s and 1990s. During these tests, various U, Pu and Zr contents and various cladding types were examined. Typically, the post irradiation examination focused on cladding endurance limits, fuel column elongation, fission-gas release, cladding strain, fuel microstructure, and fuel/cladding interaction.

Based on the irradiation of these metal fuels, a number of fast reactor metal fuel performance codes were developed including SIEX4[4], FEAST-Metal[8], and LIFE-Metal[12]. Under this work, correlations were primarily taken from SIEX4 and FEAST-Metal as well as several other sources.

In addition to the data that has previously been taken in order to qualify a fuel performance code to perform safety analyses, one important piece of information not available is online measurements of fuel temperature during irradiation. This could be used to validate the code predictions of fuel temperature, as well as validate temperature-dependent models, which are a primary driver for many of the fuel performance mechanisms.

3. Properties and Models Added to FAST

A number of material properties for U-Pu-Zr fuel and HT9 cladding have been added to FAST. Additionally, a number of other fuel performance models were necessary to model the EBR-II rods. These properties and models are described in this section.

3.1. U-Pu-Zr Material Properties

The fuel material properties that have been added to FAST to allow for the modeling of the selected EBR-II rods are described in this section and include thermal expansion, thermal conductivity, melting temperature, fuel/cladding eutectic temperature, density, and swelling. UO₂ pellets exhibit in-reactor densification, because they are a sintered product. The metal fuels are not sintered and no further in-reactor densification is included. Heat capacity is not needed for the steady-state calculations that are performed for these fuel rods, but would be necessary for transient fuel calculations. Finally, all the fuel rods that are modeled have liquid sodium in the fuel-clad gap, and therefore, no emissivity properties for the fuel or cladding are necessary as there will not be any radiation heat transfer.

The thermal expansion of U-Pu-Zr fuel is a function of temperature and is taken from data from [4] and is valid between 273K and 1213K.

$$\begin{aligned} \frac{\Delta L}{L} &= 1.76 \times 10^{-5}(T - 298) & T < 868\text{K} \\ \frac{\Delta L}{L} &= 1.003 \times 10^{-2} + 7.43 \times 10^{-5}(T - 868) & 868\text{K} < T < 938\text{K} \\ \frac{\Delta L}{L} &= 1.52 \times 10^{-2} + 2.01 \times 10^{-5}(T - 938) & T > 938\text{K} \end{aligned}$$

Where:

$\Delta L/L$ = Thermal expansion (m/m)
 T = Temperature (K)

The thermal conductivity of U-Pu-Zr fuel is a function of temperature, Pu content, Zr content, and porosity and is taken from data from [4] and is valid between 273K and 1000K.

$$k = \frac{D_1}{100} \left(AT + \frac{BT^2}{2} + \frac{CT^3}{3} \right)$$

$$D_1 = \frac{1 - P}{1 + 2 \cdot P}$$

$$A = 17.5 \left(\frac{1 - 2.23 \cdot Zr}{1 + 1.61 \cdot Zr} - 2.62 \cdot Pu \right)$$

$$B = 0.0154 \left(\frac{1 + 0.061 \cdot Zr}{1 + 1.61 \cdot Zr} + 0.9 \cdot Pu \right)$$

$$C = 9.38 \times 10^6 (1 - 2.7 \cdot Pu)$$

Where:

k = Thermal conductivity (W/m-K)
 T = Temperature (K)
 P = fraction of porosity in the fuel (fraction)
 Zr = weight fraction of fuel that is zirconium (fraction)
 Pu = weight fraction of fuel that is plutonium (fraction)

The melting temperature of U-Pu-Zr fuel is a function of Pu content and Zr content and is taken from [4]. The fuel/cladding eutectic temperature is also taken from [4].

$$T_{melt} = 1132(1 - 0.77 \cdot Pu)(1 - 0.94 \cdot Zr) + 273.15$$

$$T_{eutectic} = 973$$

Where:

T_{melt} = Fuel melting temperature (K)
 $T_{eutectic}$ = Fuel/cladding eutectic temperature (K)
 P = fraction of porosity in the fuel (fraction)
 Zr = weight fraction of fuel that is zirconium (fraction)

The theoretical density of U-Pu-Zr fuel is taken to be 15.8 g/cm³. The user has the ability to input the fraction of theoretical density of the fuel, which for the metallic fuels used in EBR-II was typically in the 70-80% range (compared to 96-97% for today's UO₂ fuels).

There is considerable difference in recommendations for the fission product swelling of U-Pu-Zr fuel. It is clear that there is a lower swelling rate after fuel/clad gap is closed. For this modeling effort, the swelling rates before and after the gap is closed are taken as a function of burnup to provide reasonable estimate of the measured cladding strain.

$$\frac{\Delta V}{V} = 0.05 \cdot Bu \quad \text{Fuel/clad gap open}$$

$$\frac{\Delta V}{V} = 0.009 \cdot Bu \quad \text{Fuel/clad gap closed}$$

Where:

$\frac{\Delta V}{V}$ = Fuel volumetric swelling (fraction)
 Bu = Burnup (atom%)
 (note: 1 GWd/MTM = 0.1066 at%)

3.2. HT9 Material Properties

The cladding material properties that have been added to FAST to allow for the modeling of the selected EBR-II rods are described in this section and include, thermal expansion, thermal conductivity, density, elastic moduli, and creep. Negligible void swelling has been observed in HT9 to high fast neutron fluence [5], so no irradiation growth is assumed. Heat capacity is not needed for the steady-state calculations that are performed for these fuel rods, but would be necessary for transient fuel calculations. Finally, the yield stress of the cladding is not necessary for the steady-state calculations that are performed for these fuel rods as all cladding deformation will be in the elastic range and permanent deformation will be via creep rather than plastic slip. For the modeling of rapid transients with significant pellet/clad mechanical interaction, the yield stress and cladding plastic behavior would be necessary.

The thermal expansion of HT9 cladding is a function of temperature and is taken from data from [6] and is valid between 273K and 1073K.

$$\frac{\Delta L}{L} = 1.842 \times 10^{-9} \cdot T^2 + 9.226 \times 10^{-6} \cdot T - 2.882 \times 10^{-3}$$

Where:

$$\begin{aligned} \Delta L/L &= \text{Thermal expansion (m/m)} \\ T &= \text{Temperature (K)} \end{aligned}$$

The thermal conductivity of HT9 cladding is a function of temperature and is taken from data from [7] and is valid between 273K and 873K.

$$k = 4.397 \times 10^{-3} \cdot T - 2.247 \times 10^1$$

Where:

$$\begin{aligned} k &= \text{Thermal conductivity (W/m-K)} \\ T &= \text{Temperature (K)} \end{aligned}$$

The density of HT9 cladding is taken to be 7.75 g/cm³. The cladding is assumed to be at its theoretical density.

The Young's modulus and shear modulus of HT9 cladding is a function of temperature and is taken from data from [8] and is valid between 273K and 873K.

$$\begin{aligned} E &= 213.7 - 0.10274 \cdot (T - 273.15) \\ G &= 89.64 - 0.05378 \cdot (T - 273.15) \end{aligned}$$

Where:

$$\begin{aligned} E &= \text{Young's modulus (GPa)} \\ G &= \text{Shear modulus (GPa)} \\ T &= \text{Temperature (K)} \end{aligned}$$

The creep rate of HT9 cladding is a function of temperature, fast neutron flux and stress is taken from [9] and is valid between 273K and 1000K. The creep rate is composed of irradiation creep rate and thermal creep rate. In most in-reactor applications, the irradiation creep rate is dominant.

$$\begin{aligned} \dot{\epsilon}_{irrad} &= 10^7 \left(B_0 + A_1 \exp\left(\frac{-Q}{RT}\right) \right) \phi \sigma_{eff}^{1.3} \\ \dot{\epsilon}_{therm} &= \dot{\epsilon}_1 + \dot{\epsilon}_2 + \dot{\epsilon}_3 \\ \dot{\epsilon}_1 &= \left(C_1 \exp\left(\frac{-Q_1}{RT}\right) \sigma_{eff} + C_2 \exp\left(\frac{-Q_2}{RT}\right) \sigma_{eff}^4 + C_3 \exp\left(\frac{-Q_3}{RT}\right) \sigma_{eff}^{0.5} \right) C_4 \exp(-Q_4 t) \end{aligned}$$

$$\dot{\epsilon}_2 = C_5 \exp\left(\frac{-Q_4}{RT}\right) \sigma_{eff}^2 + C_6 \exp\left(\frac{-Q_5}{RT}\right) \sigma_{eff}^5$$

$$\dot{\epsilon}_3 = 4 \left(C_7 \exp\left(\frac{-Q_6}{RT}\right) t \right)^3 \sigma_{eff}^{10}$$

Where:

$\dot{\epsilon}_{irrad}$	=	Effective irradiation strain rate (%/sec)
$\dot{\epsilon}_{therm}$	=	Effective thermal strain rate (%/sec)
$\dot{\epsilon}_1$	=	Effective thermal primary strain rate (%/sec)
$\dot{\epsilon}_2$	=	Effective thermal secondary strain rate (%/sec)
$\dot{\epsilon}_3$	=	Effective thermal tertiary strain rate (%/sec)
σ_{eff}	=	Effective stress (MPa)
T	=	Temperature (K)
ϕ	=	Fast neutron flux (n/cm ² /s x 10 ⁻¹⁵)
B ₀	=	1.83 × 10 ⁻⁴
A	=	2.59 × 10 ¹⁴
Q	=	73000
R	=	1.987
C ₁	=	1.34 × 10 ¹
C ₂	=	8.43 × 10 ⁻³
C ₃	=	4.08 × 10 ¹⁸
C ₄	=	1.60 × 10 ⁻⁶
C ₅	=	1.17 × 10 ⁹
C ₆	=	8.33 × 10 ⁹
C ₇	=	2.12 × 10 ⁷
Q ₁	=	1.5 × 10 ⁴
Q ₂	=	26451
Q ₃	=	89167
Q ₄	=	83142
Q ₅	=	108276
Q ₆	=	94233.3

(note: effective stress is about equal to hoop stress divided by 1.155 and effective strain is about equal to hoop strain times 1.155)

3.3. Other Fuel Performance Models

Other models necessary for modeling EBR-II fuel have been included in FAST. These include; fission gas release, gap conductivity of sodium-filled gap, plenum filling, radial power profile, burnup calculations, and sodium coolant heat transfer properties.

The fission gas release from U-Pu-Zr fuel is a constant fraction of the produced gas taken from [4]. A value of 70% is used for nominal predictions and a value of 85% is used for conservative predictions. This constant release fraction is a very crude modeling approach, and it is acknowledged that a diffusional release model would be preferable. However, the data needed for such model development does not currently exist. Other codes such as FEAST-Metal use a fitted release curve as a function of burnup, but this approach does not seem appropriate as it ignores the possible impact of power level and temperature on fission gas release and was only developed based on a few data at similar power levels.

The conductivity of the sodium-filled gap is a function of the gap size and the sodium conductivity, which is a function of temperature. This model is taken from [4].

$$H_{gap} = \frac{k_{sodium}}{r_c \cdot \ln\left(\frac{r_c}{r_f}\right)}$$

$$k_{sodium} = 93 - 5.81 \times 10^{-2}(T + 273) + 1.173 \times 10^{-5}(T + 273)^2$$

Where:

H_{gap}	=	Gap conductance (W/m ² -K)
k_{sodium}	=	Sodium thermal conductivity (W/m-K)
T	=	Temperature (K)
r_c	=	radius of cladding inner surface (m)
r_f	=	radius of fuel outer surface (m)

To determine the plenum volume of the fuel rod at each time step, the initial plenum volume is reduced by the volume of sodium displaced by the fuel/cladding gap closing. Additionally, during the open gap condition, the fuel is allowed to swell axially into the plenum.

The radial power profile is set as constant across the radius at all burnup levels. The flat power profile expected in liquid metals reactor (LMR) fuel was confirmed using MCNP6.1 [10] and Serpent 2.1.28 [11]. The compositions and power histories of pins in three assemblies (X425, X430, and X447) were utilized in MCNP and Serpent to tally fission reaction rates as a surrogate to power in twenty equal area rings in the fuel. Temperatures were approximated for both codes with the fuel modeled at 900 °C, and the clad and sodium modeled at 600 °C. The flat radial power profile within a single reflected pin occurs due to the mean free path of fast neutrons being longer in LMR fuel than LWR fuel. This results in LMR fuel not having the characteristic edge peaking seen in LWR fuel pins. The recommended radial profile is flat with normalized power values in each fuel ring equal to 1.0.

The burnup increment for each time step is determined by multiplying the local LHGR by the time step size. By dividing by the fuel cross-sectional area and the fuel apparent density the burnup in GWd per metric ton fuel can be determined. By further dividing by 1 minus the zirconium weight fraction the burnup in GWd per metric ton heavy metal (MTM) can be determined. As previously mentioned, assuming 200 MeV per fission, 1GWd/MTM=0.1066 atom %.

The sodium coolant properties are taken from [13] and the heat transfer coefficient is determined using the Schad and Subbotin correlations [14].

4. EBR-II Rods

Three EBR-II fuel assemblies were used in this modeling exercise. They are X425, X430, and X447. These rods were selected because they were used in the assessment of FEAST-Metal [8] and fabrication, operational, and post-irradiation data were readily available. Fuel information for rods from each assembly is shown in Table 1. Power histories for the rods selected from each assembly are shown in Figure 1. The same axial power profile is used for all three rods. A FAST input file was developed for a representative rod in each assembly.

Table 1: Fuel information for EBR-II assemblies

	X425	X430	X447
<i>Fuel rod design</i>			
Plenum to fuel ratio	1	1.4	1.4
Fuel outer radius	2.16 mm	2.858 mm	2.2 mm
Clad inner radius	2.539 mm	3.277 mm	2.54 mm
Clad outer radius	2.92 mm	3.683 mm	3.92 mm
Pu fraction	19 wt%	19 wt%	0 wt%
Zr fraction	10 wt%	10 wt%	10 wt%
Smear density	72.4%	76.1%	75%
Initial fill gas pressure	84000 Pa	84000 Pa	84000 Pa
Bond sodium height above fuel	6.35 mm	6.35 mm	6.35 mm

Fuel slug total length	343 mm	343 mm	343 mm
Cladding	HT9	HT9	HT9
Reactor conditions			
Coolant pressure	100,000 Pa	100,000 Pa	100,000 Pa
Fuel rod pitch	7.59 mm	9.58 mm	7.59 mm
Coolant velocity	0.0565 kg/s	0.07 kg/s	0.0339 kg/s
Coolant mass flux	1830 kg/m ² -s	1430 kg/m ² -s	1100 kg/m ² -s
Coolant inlet temperature	370°C	370°C	370.85°C
Ratio of fast neutron flux (n/m ² /s) to specific power (W/g)	1 × 10 ¹⁷	1 × 10 ¹⁷	1 × 10 ¹⁷

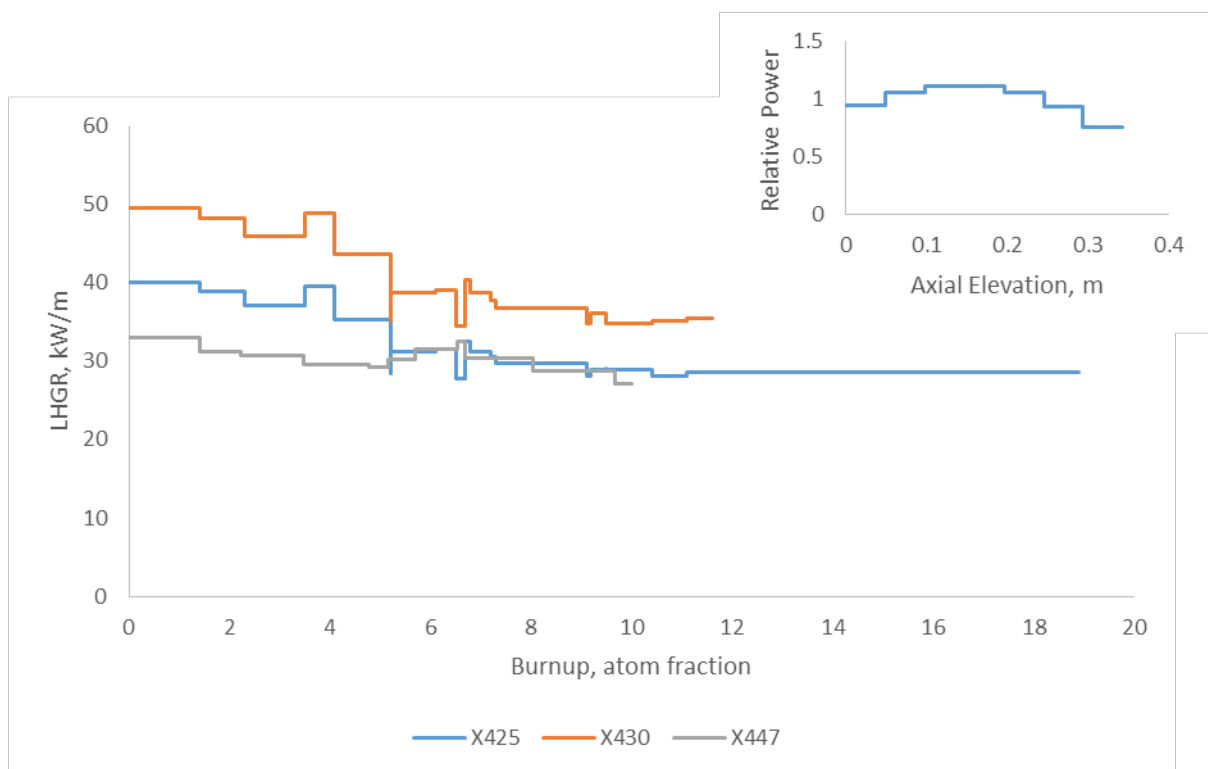


Figure 1. Power histories for selected rods from EBR-II assemblies. The same axial power profile was used for each rod.

5. Model Predictions and Comparison to Data

Fission gas release and cladding strain data are available for each of the rods that were modeled. In addition there are data regarding the sodium heat-up along the length of the rod at various power levels. In this section, comparisons to these data are made to determine how well FAST predicts these data. These data will help assess the ability of FAST to predict rod internal pressure which is primarily driven by fission gas release, cladding strain capability, and sodium coolant heat transfer. It is acknowledge that this is a limited assessment but makes use of the currently available data. Also of regulatory interest would be a measurement of online fuel temperature to compare FAST predictions to. Such measurements should be the focus of future experiments.

A representative safety analysis is performed for one of these rods to demonstrate the ability of FAST to perform these calculations. Due to a lack of experimental data, these calculations

cannot be fully validated, however, following each safety analysis calculation, the experimental data required to validate the code prediction will be identified. This information could be used to direct future irradiation tests to obtain data required to validate a safety analysis.

5.1. Comparisons to data

The predicted sodium outlet temperature was compared to the measured sodium outlet temperature for each of the three rods. In all cases, there was excellent agreement with a standard error of 3.1°C. The measured and predicted outlet temperatures are shown in Figure 2. This demonstrates that the sodium heat transfer correlations are working properly.

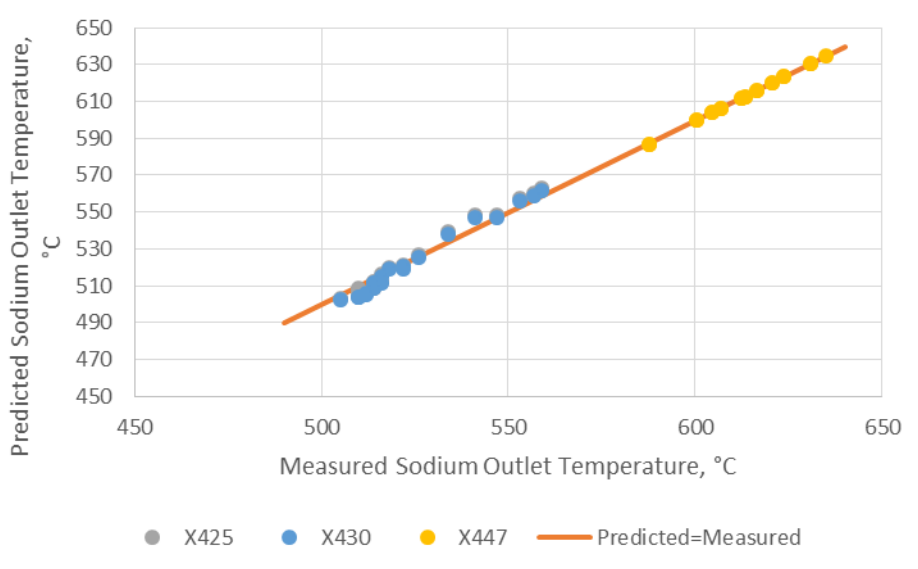


Figure 2. Measured vs. predicted sodium outlet temperatures.

5.1.1. Rod X425

FAST predictions of fission gas release are shown in Figure 3 along with measured data. The cladding strain predictions are shown in Table 2 for the peak strain at various burnup levels and in Figure 4 as a function of axial elevation for a given burnup. These comparisons show that the fission gas release predictions are reasonable. The cladding strain is also predicted reasonably within $\pm 0.3\%$ strain.

FAST predicts the heatup of the sodium coolant along the length of the rod well in comparison with the data as well as the burnup levels.

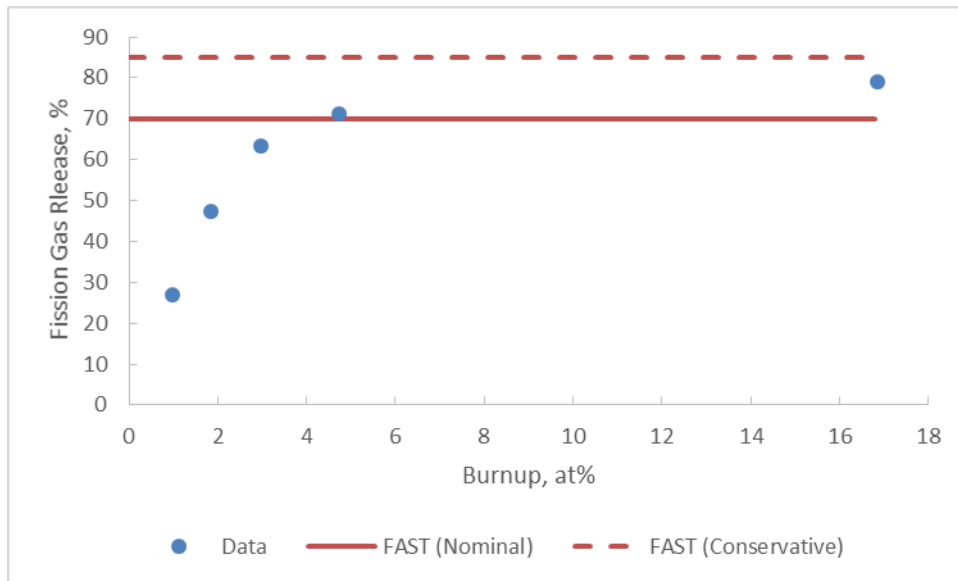


Figure 3. Measured and predicted fission gas release from X425.

Table 2: Measured and predicted peak cladding permanent hoop strain from X425 as a function of burnup

Burnup at%	Measured Strain, %	Predicted Strain, %
10.4	0.25	0.10
15.8	0.98	1.26
18.9	2.0	1.99

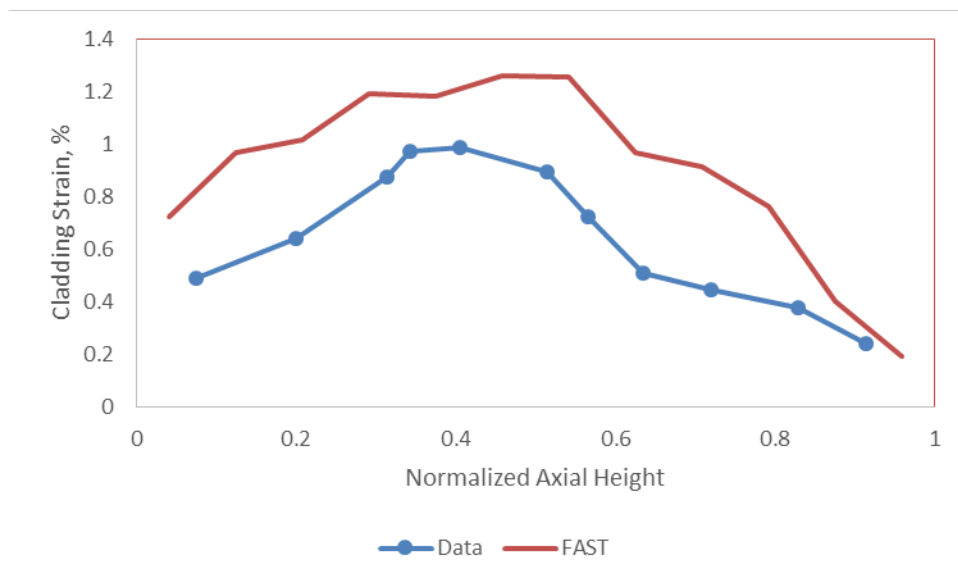


Figure 4. Measured and predicted cladding permanent hoop strain from X425 at 15.8 at% burnup as a function of axial elevation.

5.1.2. Rod X430

FAST predictions for fission gas release for rod X430 are shown in Figure 5 along with measured data. The cladding strain predictions are shown in Table 3 for the peak strain at various burnup levels. This comparison shows that the fission gas release predictions are reasonable. The cladding strain is also predicted reasonably with some under prediction between 0.2 and 0.4% strain.

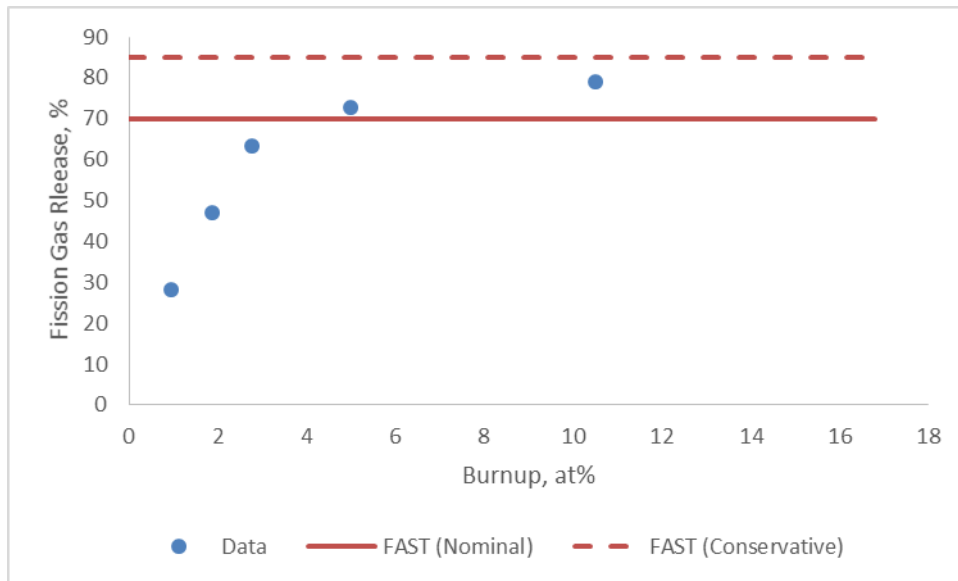


Figure 5. Measured and predicted fission gas release from X430.

Table 3: Measured and predicted peak cladding permanent hoop strain from various rods in assembly X430 as a function of burnup

Burnup at%	Measured Strain, %	Predicted Strain, %
7.3	0.28, 0.38, 0.28	0.10
11.8	0.97, 0.86, 1.17, 1.03	0.75

5.1.3. Rod X447

FAST predictions of fission gas release for rod X447 are shown in Figure 6 along with measured data. This comparison shows that the fission gas release predictions are reasonable. For this rod, the measured cladding strain around the middle of the rod was around 0.4-0.5% and FAST predicted 0.32% which is an under prediction of less than 0.2% strain.

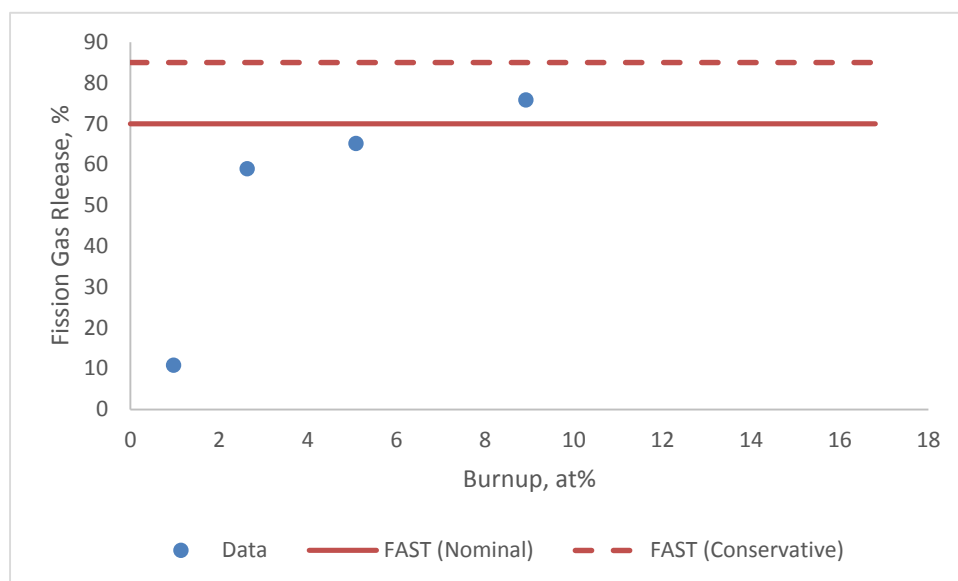


Figure 6. Measured and predicted fission gas release from X447.

5.2. Sample Safety Analysis Calculations

Sample safety analysis calculations are performed for one of the EBR-II X-430. This rod was selected as it had the highest power. However, when performing each of these analysis, typically a methodology is developed to identify the limiting rod for each analysis.

All the safety analyses that are typically performed for LWR fuel are not performed in this case. Rod internal pressure is not evaluated as these rods are designed with very large plenum space to accommodate the release of all the fission gas. Strain is reasonably predicted by FAST, but it is not well known what the strain limit would be.

The one safety analysis calculation that can be performed is the power required to melt the fuel at the pellet centerline or cause the fuel cladding eutectic temperature to be exceeded. By increasing the power incrementally, it was found that a power level of 60.4 kW/m (18.4 kW/ft) will cause the fuel/cladding interface to exceed the eutectic temperature of 973K. At this power level the fuel centerline is still below the fuel melting temperature. Therefore it can be seen that the fuel/cladding eutectic temperature is more limiting than the fuel melting temperature for this rod. Online fuel centerline temperature and fuel/clad bond temperature measurements would be critical to assess code predictions of the power resulting in fuel melting and exceeding fuel/cladding eutectic temperature.

6. Conclusions and Future Work

This paper has demonstrated the ability of the FAST fuel performance code to adequately model metal fuel irradiated in EBR-II. Comparisons to sodium outlet temperature data were excellent which demonstrates that the boundary conditions are correctly modeled. Comparisons to fission gas release and cladding strain were reasonable. At low burnup the crude fission gas release model over predicts the fission gas release, but later in life provides adequate predictions. For the cladding strain, the predicted strains were within less than $\pm 0.4\%$ strain. In order to adequately validate safety analyses that would be performed on such a fuel, various data would be needed including, power ramp data, HT9 strain capability and fatigue data, rod-internal pressure limit, and in-reactor centerline temperature measurements.

As noted earlier, there is work to be done before FAST is ready for use by the NRC to perform safety evaluations for metallic fuels. Two significant areas of model development needed are refining the fission gas release model, and evaluating the need and impacts of a zirconium-redistribution model in the metallic fuel. In addition, significant more assessment is needed to quantify the uncertainty in the phenomena of interest in FAST. However, even more importantly, it must be understood what the licensing criteria and/or specified acceptable fuel design limits (SAFDLs) are in order to determine what are the models and phenomena of interest. As FAST is a tool used for safety analysis and not for design, it is important that the models and assessment revolve around those that impact safety.

7. References

1. Geelhood KJ, WG Luscher, PA Raynaud, IE Porter. 2015. *FRAPCON-4.0: A Computer Code for the Calculation of Steady-State, Thermal-Mechanical Behavior of Oxide Fuel Rods for High Burnup*. PNNL-19418, Vol. 1 Rev. 2, Pacific Northwest National Laboratory, Richland, Washington
2. Geelhood KJ, WG Luscher, JM Cuta, IE Porter. 2016. *FRAPTRAN-2.0: A Computer Code for the Transient Analysis of Oxide Fuel Rods*. PNNL-19400, Vol.1 Rev2, Pacific Northwest National Laboratory, Richland, Washington
3. Porter, IE, KJ Geelhood. 2018. *FAST-1.0: A Computer Code for the Calculation of Steady-State and Transient Thermal-Mechanical Behavior of Oxide Fuel Rods*. Publication Pending, U.S. Nuclear Regulatory Commission, Washington DC.

4. R.B. Baker, and D.R. Wilson, 1992, SIEX4 - A Correlated Computer Code for Prediction of Fast Reactor Fuel and Blanket Pin Performance, WHC-SP-0865 Rev.0, Westinghouse Hanford Company, Richland, WA
5. Y. Chen, 2013 "Irradiation Effects of HT-9 Martensitic Steel", NUCLEAR ENGINEERING AND TECHNOLOGY, VOL.45 NO.3 JUNE 2013.
6. N. Yamanouchi, M. Tamura, H. Hayakawa, A. Hishinuma and T. Kondo, J. Nuclear Materials, v191-194, p822 (1992)
7. M. Akiyama, Design of Fusion Reactors, Pub. World Scientific, (1991), p462
8. A. Karahan, 2007 "Modeling of Thermo-Mechanical and Irradiation Behavior of Metallic and Oxide Fuels for Sodium Fast reactors", Doctor of philosophy in nuclear science and engineering at the Massachusetts Institute of Technology
9. Letter, R. j_ Puigh to G. D. Johnson, Creep Equation for 10.5 Cr-1.5 Mo Ferritic Steel, dated March 17, 1987.
10. T. Goorley, et al., 2012 "Initial MCNP6 Release Overview", *Nuclear Technology*, **180**, pp 298-315.
11. J. Leppänen. 2015 *Serpent – a Continuous-energy Monte Carlo Reactor Physics Burnup Calculation Code*. VTT Technical Research Centre of Finland.
12. M. C. Billone, et al., 1986, "Status of the Fuel Element Modeling Codes for Metallic Fuels," Proc. Int. Conf. Reliable Fuels for Liquid Metal Reactors, American Nuclear Society Tucson, Arizona.
13. Fink, J.K. and L. Leibowitz. 1995. *Thermodynamic and Transport Properties of Sodium Liquid and Vapor*. Reactor Engineering Division ANL/RE-95/2 Report. Argonne National Laboratory.
14. Ha, K.S. et. al., 2007 "Development of MARS-LMR and Steady-state Calculation for KALIMER-600", KAERI/TR-3418/2007